

**Molecular Engineering of Stimuli-Responsive, Functional,
Side-Chain Liquid Crystalline Copolymers: Synthesis,
Properties and Applications**

Journal:	<i>Polymer Chemistry</i>
Manuscript ID	PY-REV-05-2020-000749.R1
Article Type:	Review Article
Date Submitted by the Author:	12-Aug-2020
Complete List of Authors:	Ndaya, Dennis; University of Connecticut, Department of Chemistry Bosire, Reuben; University of Connecticut, Department of Chemistry Vaidya, Samiksha; University of Connecticut, Department of Chemistry Kasi, Rajeswari; University of Connecticut, Chemistry and Polymer Program, IMS

Molecular Engineering of Stimuli-Responsive, Functional, Side-Chain Liquid Crystalline Copolymers: Synthesis, Properties and Applications

Dennis Ndaya^{‡#}, Reuben Bosire^{‡#}, Samiksha Vaidya[†] and Rajeswari M. Kasi^{†§*}

[†]Department of Chemistry, University of Connecticut, Storrs, CT 06269 (USA)

[§]Polymer Program, Institute of Material Science, University of Connecticut, Storrs, CT 06269 (USA)

Equal Contribution *Principal Investigator

*Authors to whom correspondence should be addressed.

Prof. R M Kasi: rajeswari.kasi@uconn.edu; Tel: +1 (860)-486-4713

ABSTRACT

This review describes recent progress made in designing stimuli-responsive, functional, side-chain, end-on mesogen attached liquid crystalline polymers (LCPs). Developments in synthetic methodologies including controlled and living techniques provides an easy access to well-defined liquid crystalline polymers. For example, the synthesis of linear liquid crystalline block copolymers (LCBCPs), block copolymers with a linear, coil-coil, non-LC block and an end-on mesogen attached LC block, provides a route to polymers with morphology and properties akin to conventional block copolymer. However, synthesis of topologically branched LCBCPs with a branched coil-coil non-liquid LC block and an end-on mesogen attached LC block is used to manipulate phase behavior, morphology and alignment kinetics of the resultant polymer. Furthermore, synthesis of branched liquid crystalline random copolymers wherein the branched coil-coil non LC unit and end-on mesogen LC unit are statistically distributed results in never-before-seen helical and curved interfaces with new and enhanced properties. Finally, synthetic strategies to incorporate organic dye molecules into a variety of liquid crystalline polymer frameworks produces new optically active and adaptive soft materials. In the outlook section, the need for topologically-diverse synthetic as well as naturally derived liquid crystalline polymer architectures along with processing tools and field directed assemblies to produce functional materials and their applications are discussed.

ABBREVIATIONS

LC: Liquid crystals

LCP: Liquid crystalline polymers

BCP: Block copolymers

LCBCP: Liquid crystalline block copolymers

SmA: Smectic mesophase

SmA*: Chiral smectic A mesophase

SmC: Tilted smectic C mesophase

SmC*: Tilted chiral smectic C mesophase

N: Nematic mesophase

N* or Ch*: Cholesteric, chiral helical or chiral nematic mesophase

IMDS: Intermaterial dividing surface

PSLC: Polymer stabilized liquid crystals

CLC: Cholesteric liquid crystals

Section 1: Introduction

Control of polymeric self-assembly by exploiting molecular and supramolecular interactions is a useful strategy to create hierarchical functional materials. To create responsive and functional polymeric assemblies, liquid crystalline mesogens and non-liquid crystalline moieties are incorporated a block-like or statistically random arrangement.^{1,2} This result in liquid crystalline block copolymers or liquid crystalline random copolymers, respectively, Figure 1.

Coil-coil linear liquid crystalline block copolymers (LCBCPs), wherein the non-LC block is topologically linear and the LC block has end-on LC attachment (side-chain), is a well-studied model system. These LCBCPs exhibit hierarchical order due to the microphase separation in the length scale of 10–100 nm and temperature-dependent thermotropic LC mesophase ordering in the length scale of 3–10 nm, Figure 2.³⁻⁶ Microphase segregated structures on the length scale of 10–100 nm may form spherical, cylindrical, gyroid, and lamellar morphologies dependent on (i) volume fraction of the different blocks with LCBCPs and (ii) incompatibility factor between the competing blocks.⁷⁻¹¹ Furthermore, liquid crystalline mesophase morphology is dependent on orientation order, positional order, molecular shape, topology and amphiphilicity of the LC molecules such that conventionally: i) nematic phases are formed by rod-like or disc-like units that have long range orientational order; ii) cholesteric phases, which reflect visible light, are formed by chiral nematic mesogens; iii) smectic mesophases are formed when rod-like molecules arrange in layers; iv) columnar mesophases are formed by disc-like molecules that arrange in a column, Figure 2.^{1-3, 6} However, in LCBCPs, the interplay between microphase segregation and LC order has a strong influence on the resulting self-assembled structure, mesophase, thermal and morphological properties as well as block copolymer order-disorder transition temperature, Figure 2.^{3, 12-14} In most cases, microphase segregation of the block architecture dominates, followed by parallel or perpendicular anchoring of LC molecules to the intermaterial dividing surface (IMDS).^{2, 15, 16} This determines interfacial curvature, which in turn impacts microphase segregated (10-100 nm) and LC mesophase (3-7 nm) nanostructured morphology.^{3, 6, 17} More importantly, and until very recently, due to the very high surface-to-volume ratio at the IMDS, only smectic LC layers (SmA, SmC*) or nematic (N) mesophases are favored.^{3, 18}

Most research on coil-coil LCBCPs are focused on systems comprising linear amorphous or linear semicrystalline polymers as the non-LC block and side-chain LC units in the other block.^{19, 20} For example, LCBCPs comprising linear semicrystalline PEO in one block and side-on LC mesogen in the other block have been well-studied.²¹⁻²³ Herein, the interplay of LC order, crystallization of PEO and microphase segregation of the block architecture on the formation of unique morphologies have been well-documented and used to create ion conducting electrochemical devices and batteries.²³ However, in many of these examples, the order-disorder transition temperature of the LCBCPs is very high, making it difficult to process the LCBCPs and to attain long-range order. To overcome these issues, several different approaches are used including (1) synthesis of non-linear topologies such as branched, brush-like or comb-like non-LC molecules on the self-assembly and the processing of LCBCPs^{24, 25} and (2) utilization of the diamagnetic property of the LC phase above the order-disorder transition temperatures to align both the LC mesophase and the non-LC microphase segregated structures by using a magnetic field.²⁶⁻²⁸ Thus, the field of LCBCPs has undergone a lot of development in the synthesis and the structure-property-processing areas to advance the use of these materials. Furthermore, in the

recent years molecular engineering of new topologies of non-LC units within random liquid crystalline copolymers in conjunction with processing tools are being developed to fully explore the interplay of self-organizing LC and branched non-LC units to design the next generation of materials.²⁹

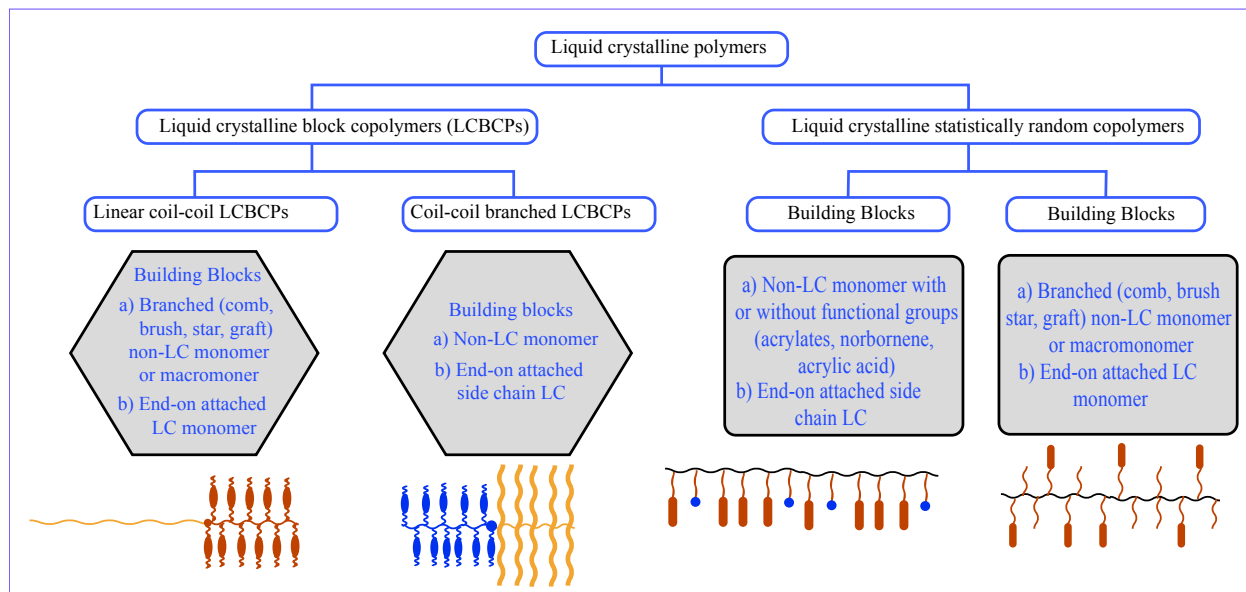


Figure 1: Thermotropic liquid crystals attached as end-on type side chains within block copolymer framework (linear and branched LCBCPs) and statistically random copolymer framework (linear and branched random LCPs).

Section 2: Liquid crystalline mesogens

There are many libraries of small-molecule liquid crystalline mesogens that have been developed in the past hundred years starting with the preparation of pure cholesteryl ester.² In this Review, we will focus on cholesterol, azobenzene, cyanobiphenyl and benzoate building blocks as end-on, side-chain mesogens within LCPs, Figure 3. Cholesterol is a chiral molecule with planar rigid structure, that selectively reflects light in the visible range (400-800 nm) and can be used as a photonic band gap material.^{30, 31} Cholesteryl moieties can be attached to different monomers including acrylates, methacrylates, siloxanes, norbornenes, and lactones.³¹⁻³⁴ These monomers are polymerized by controlled radical, ring opening and ring opening metathesis polymerization methods to produce LC homo-, random and block copolymers.³² Other important LC mesogens typically used are cyanobiphenyl³⁵, alkoxy benzoic acid³⁶, benzoates³³ and azobenzene^{37, 38} derivatives.

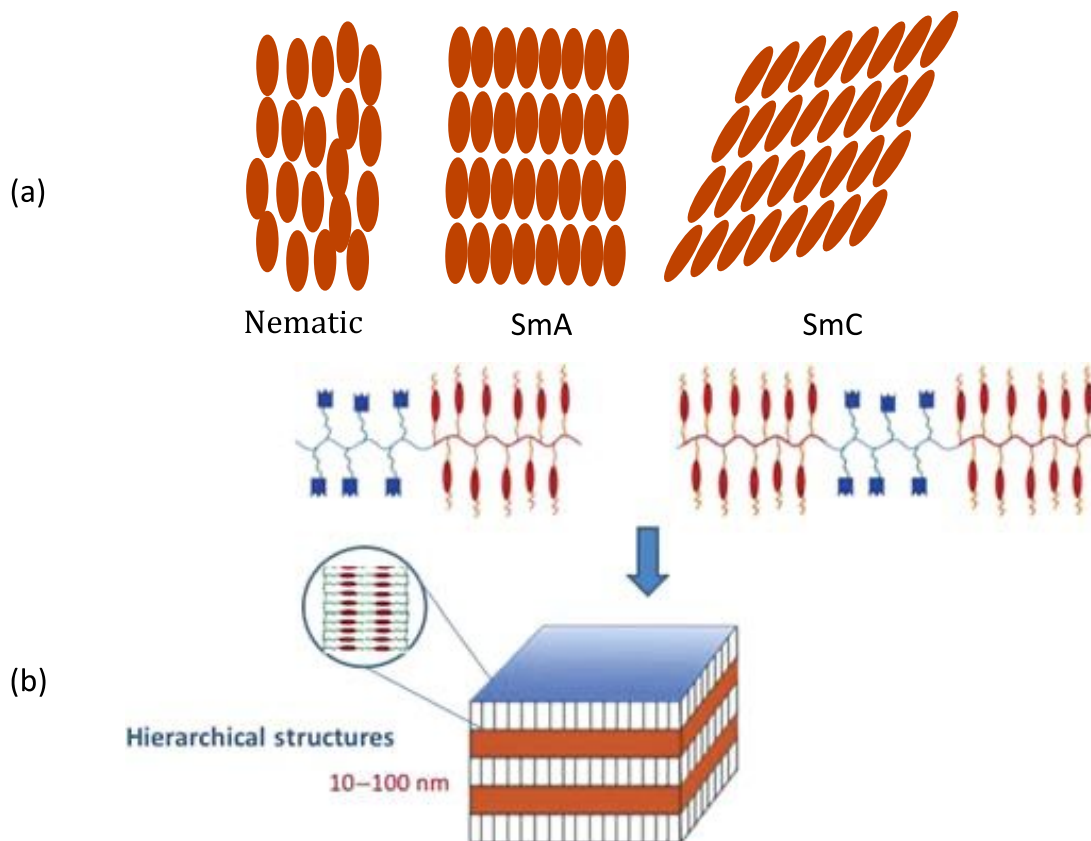


Figure 2. (a) Liquid crystalline mesophases. (b) An example of hierarchical structure from diblock and triblock copolymers containing side-chain liquid crystals. Conventional hierarchical self-assembly of liquid crystalline block copolymers result in liquid crystal order (1-10 nm) and block copolymer microphase segregation (10-100 nm). Phase transition temperatures include liquid crystalline mesophase transition temperature (T_{LCs}) and block copolymer order disorder transition temperature (T_{ODT}), which alters the intermaterial dividing surface (IMDS) and self-assembly behavior of liquid crystalline block copolymers. Shown here is a specific case wherein the liquid crystals arrange in smectic A (SmA) bilayer structures. IMDS is the interface between the red block and the blue block in this figure. Adapted with permission from Ref. 17. Copyright (2013) John Wiley & Sons, Inc.

The LC mesogens are attached to monomers via different types and lengths of spacers and (co)polymerized to yield homopolymers, statistically random copolymers and block copolymers. The type and length of spacers between mesogen and backbone is used to manipulate thermal, mesophase, optical and mechanical properties of LCPs.^{32, 34} These functional LCPs are important for LC displays, lasers, ferroelectrics, actuators, and photoresponsive materials.^{35, 39-50}

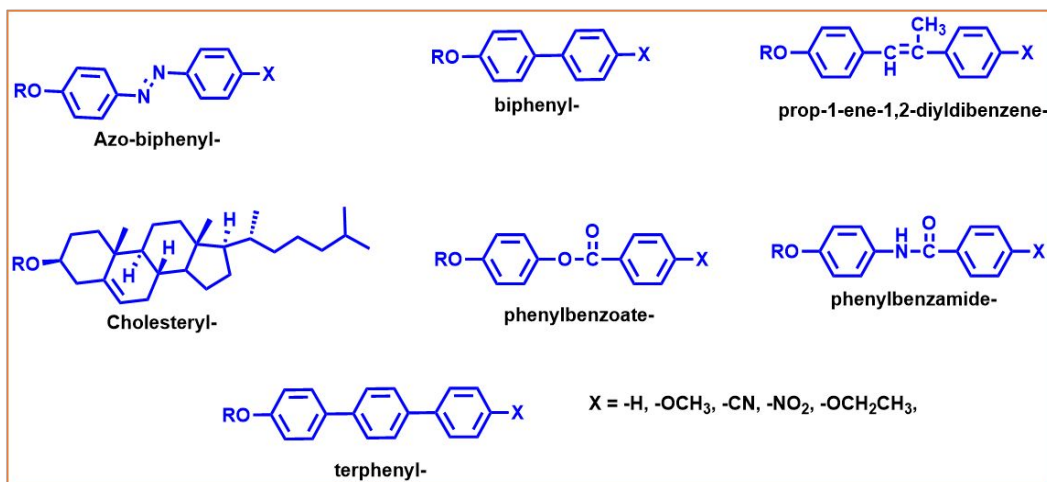


Figure 3: Chemical structures of liquid crystalline building blocks that function as end-on type mesogens.

Section 3.0: Liquid crystalline block copolymers from sequential polymerization of non-liquid crystalline monomer and end-on attached side-chain liquid crystalline monomer

As mentioned previously, conventional LCBCPs comprising linear non-LC block and side chain LC block present hierarchical structures similar to conventional coil-coil BCPs, wherein microphase segregated domains will coexist with LC mesophases.^{5, 23, 51} In many cases, microphase separated morphologies including spheres, bicontinuous gyroids, hexagonal packed cylinders, lamellae are obtained, in which LC packing is confined within the BCP microsegregated domains.^{4, 7, 23, 52} Nevertheless, the attachment of LC side groups increases the incompatibility (χ parameter) between the LC block and the non-LC block, which strengthens the BCP microphase separation.⁹ However, the conformational or structural asymmetry of dissimilar blocks due to the introduction of the side-chain mesogens and the anchoring of the mesogens to the intermaterial dividing surface (IMDS) shows deviated phase diagrams compared to that of the conventional coil-coil BCPs.^{53, 54}

Typical hierarchical structures that can be formed by LCBCPs include: (1) lamellae-in-lamellae, (2) cylinders in LC matrix and (3) LC cylinders in BCP matrix, Figure 3 and 4. (1) For the lamellae-in-lamellae structure, the mesogens form smectic layers confined within the microsegregated lamellar domains, where the LC layers are often perpendicular to the IMDS (also called homogeneous anchoring of the mesogens).^{5, 55-61} However, some also report the parallel arrangement of the LC layers with respect to the IMDS (also called homeotropic anchoring of the mesogens) where the spacer between the mesogens and the main chain are sufficiently long.⁶²⁻⁶⁴ (2) For the cylinders in the LC matrix structure, the non-LC blocks with minor volume fraction form the hexagonally packed cylinders dispersed in the matrix of smectic layers formed by LC blocks, where the director of the cylinders are usually perpendicular to the LC layers (homogeneous anchoring of the mesogens).^{21, 35, 65-67} (3) When the LC block is the majority component, LC cylinders are formed by LC layers stacking along the long axis of the cylinder with mesogens arranged parallel to the IMDS⁶⁸ and the cylinders are hexagonally packed in the matrix of non-LC block.^{17, 35, 69, 70} Other nanostructures such as nematic phase confined in

microsegregated lamellae or tilted smectic C phase in microsegregated lamellae have also been reported.⁷¹⁻⁷⁴ While hierarchical structures with specific anchoring conditions of the mesogens with respect to the IMDS can occur locally simply through the self-assembly process upon thermal annealing, long range ordering of these nanostructures are often achieved through shearing, rubbing or magnetic field alignment.^{63, 75}

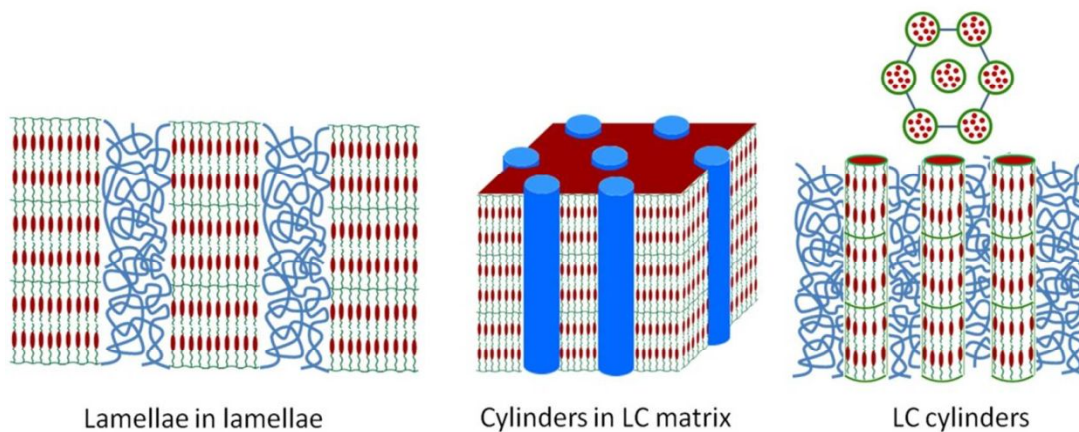


Figure 4. Different types of hierarchical structures-within-structure formed by end-on attached, side-chain, liquid crystalline block copolymers. Depending on the volume fraction of each block and the LC phase, the units may be present either in the bulk matrix or within the microphase-segregated structures. Adapted with permission from Ref. 17. Copyright (2013) John Wiley & Sons, Inc.

Several research groups are focused on developing azobenzene containing block copolymers where in azobenzene mesogens undergo trans-to-cis isomerization when exposed to photoradiation.⁷⁶⁻⁸² Here, photoisomerization is coupled with microphase segregation induced nanostructure formation. Responsive functions of these azobenzene containing LCBCPs have been harnessed for patterning nanostructures in thin films, photoresponsive elastomers, and holographic gratings.⁸³

For example, Ikeda and coworkers synthesized LCBCPs containing linear PEO in one block and side chain azobenzene in the other block, Figure 5.⁸⁴ This polymer self-assembles to form a structure of PEO cylinders dispersed in azobenzene LC matrix. This in turn increases the diffraction efficiency which is an important parameter of holographic grating.^{84, 85} BCPs containing azobenzene groups in one block helps dilute the azobenzene concentration to reduce the optical density and increase the laser permeability of the material.^{80, 81, 86} Furthermore, BCP microphase separation allows the mesogens to self-assemble within the microsegregated LC domain with cooperative effect, which otherwise would be disrupted in random copolymers.⁸⁵ They demonstrated a simple, scalable and widely application, non-contact optical method to pattern PEO cylinders, which is aligned perpendicular to the polarization of light direct and also controlled by the supramolecular cooperative motion between azobenzene LC and PEO blocks, Figure 5.⁸⁴

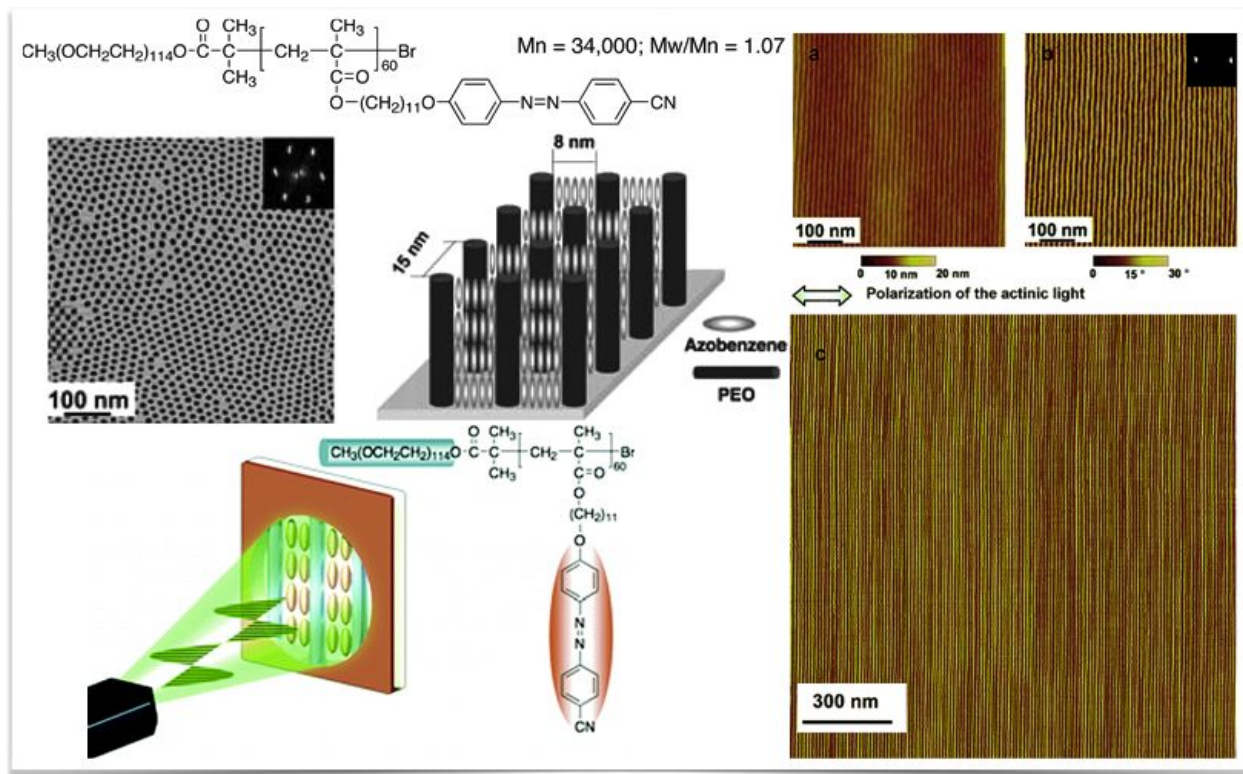


Figure 5: Azobenzene based block copolymers find applications that require photomechanical materials such as soft actuators. In this example, azobenzene is used as a molecular switch to convert input light energy into conformational change which subsequently generates strain in the polymeric materials. Trans - cis photoisomerization and trans-cis-trans reorientation of azobenzene convert input photonic energy into a mechanical output by distorting the local polymer network. Reprinted with permission from Ref. 84. Copyright (2006) American Chemical Society

Synthesis of new LCBCPs in conjunction with developments in field directed assemblies along with post polymerization reactions has been long used to produce highly ordered and aligned porous and non-porous nanostructures in thin film and in bulk for nanolithographic templates production.²⁷ Keller and Li have built on this idea and designed side-on nematic mesogens (azobenzene or benzoate derivatives) and then prepared triblock copolymers with the side-on nematogen in the central block and acrylate crosslinkable rubber units in the end block by atom transfer radical polymerization chemistry.⁸⁷ Using self-assembling bottom-up strategy, a series of photoresponsive or thermoresponsive elastomers were prepared and compared with non-crosslinked triblock copolymers.⁸⁸ The interesting nature of this LCBCP elastomer platform is reflected by the correlation of dimensional change in the nanoscopic environment and its translation into macroscopic reversible thermal actuation using the LC transition temperature as a trigger, while the actuation effect is not well-developed in the case of the non-crosslinked material. The thermoactuation and shape memory properties is controlled by degree of alignment of the LC domains using shear or magnetic field, crosslink densities as well as glass transition temperature and liquid crystalline transition temperature. The actuation response in the nanoscale is investigated by temperature-controlled X-ray measurements and correlates well with macroscopic

samples observed visually as well as dynamic mechanical analysis. This bottom up self-assembly method in conjunction with top-down lithography has been exploited to develop nano-sized to micron-sized features for the design of various devices and active surfaces.⁸⁹

There are several examples of LCBCPs comprising PEO as the non-LC block for solubilization of lithium cations for solid state polyelectrolyte applications.^{23, 52, 90-92} Some researchers prefer amorphous PEO over semicrystalline PEO because crystallization of PEO reduces the chain and segmental motion which hinders the ion transportation. Within microphase segregated PEO based LCBCP, conductivity is controlled within the amorphous PEO domains while the non-PEO LC domains provide the mechanical supporting for the amorphous PEO domains as reported.⁹² Other researchers, including Li and workers, showed that morphology can be used to parse volume, structure and dynamic effects and can be used to control ion transport.⁹¹

In another effort, using LCBCPs composed of PEO block and side-chain azobenzene block, Iyoda demonstrated that PEO domains doped with lithium salts show increased anisotropic lithium ion conductivity with perpendicularly oriented PEO cylindrical domains as ion transport channels.⁹³ Using commercial model LCBCP composed of a PEO block and a polymethacrylate block bearing side-chain cyanobiphenyl LC a next step, Osuji and coworkers utilized the diamagnetic susceptibility of cyanobiphenyl LC units to align and order microsegregated structures can be aligned by using a magnetic field of several Tesla.²⁷ This scalable processing method can result in aligned, millimeter thick BCP films containing anisotropic PEO lamellar or cylindrical domains, which show enhanced conductivity compared to the isotropic samples, Figure 6.^{26, 94-96} Osuji et al have improved this approach by using, Figure 6.^{92, 94, 97}

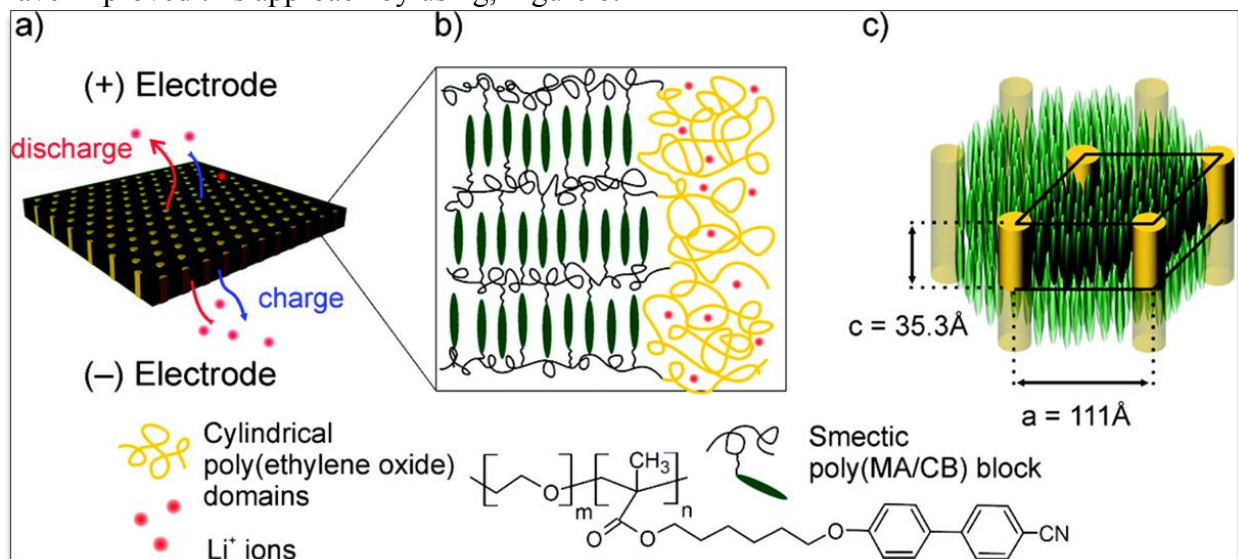


Figure 6: LCBCPs comprising PEO-b-PMA/CB forming cylindrical domains with higher conductivities when doped with Li⁺. This arrangement overcomes chain and segmental motions which hinders ion transportation. Reprinted with permission from Ref 96. Copyright (2010) American Chemical Society

Recently Osuji and coworkers have showed that self-assembly of LCBCPs in the presence of a magnetic field result in highly oriented microstructures and mesophases using low-intensity fields (<0.5 T) that are accessible using permanent magnets, in contrast to previous efforts that required high fields (>4 T) and superconducting magnets.^{26, 27} These developments provide routes to control mesophase order and produce complex textures and patterns that can be produced from commercial polymer sources.

Section 3.1: Liquid crystalline block copolymers from sequential polymerization unconventional branched non-liquid crystalline monomer (macromonomer) and end-on attached side-chain liquid crystalline monomer

LCBCPs incorporating both LC moieties and semicrystalline polymers have received great attention due to the additional structure forming phenomena (crystallization) built within the system.²³ In such systems, most research has been concentrated on the LCBCPs comprising linear semicrystalline polymers (e.g., poly(ethylene glycol), PEG) as the first block and LC units in the second block.^{19, 20, 98} However, the impact of densely grafted PEG side-chains on the structure and properties of LCBCPs have never been studied. These densely grafted brush-type polymers with unique untangled side chains are known to exhibit unprecedented self-assembled objects. Kasi and coworkers investigated the impact of LCBCP architecture comprising molecular brush-type semicrystalline PEG units in one block and side-chain LC units in the other block on hierarchical assembly and phase behavior.²⁴ They reported the synthesis of well-defined poly(norbornene)-based side-chain liquid crystalline brush block copolymers (LCBBCs) bearing cholesteryl mesogens in the first block and semicrystalline PEG in the second block, Figure 7.²⁴ Furthermore, morphologies of LCBBCs investigated by scattering and microscopic techniques reveal various hierarchical structures as a result of the interplay between the microphase segregation in brush-like macromolecules and the LC order. Finally, microphase-segregated domains dictate the anchoring of the LC mesogens at the IMDS, leading to the preferential development of smectic layers over chiral mesophases.²⁴

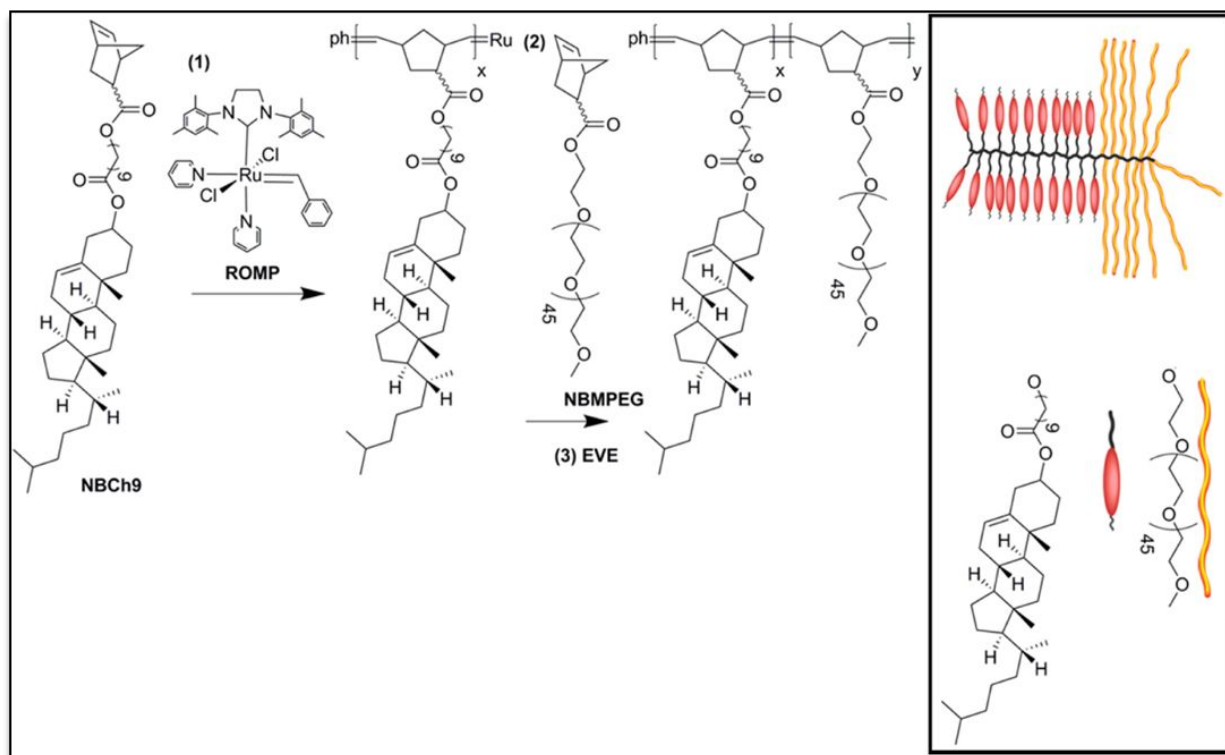


Figure 7: Synthesis of liquid crystalline brush-like block copolymers (LCBBCs). Adapted with permission from Ref. 24. Copyright (2013) American Chemical Society

Kasi, Osuji and coworkers also explored ring-opening metathesis polymerization of *n*-alkyloxy cyanobiphenyl and PLA functionalized norbornene monomers which provided precisely controlled LCBBCs, Figure 8.^{35, 99}

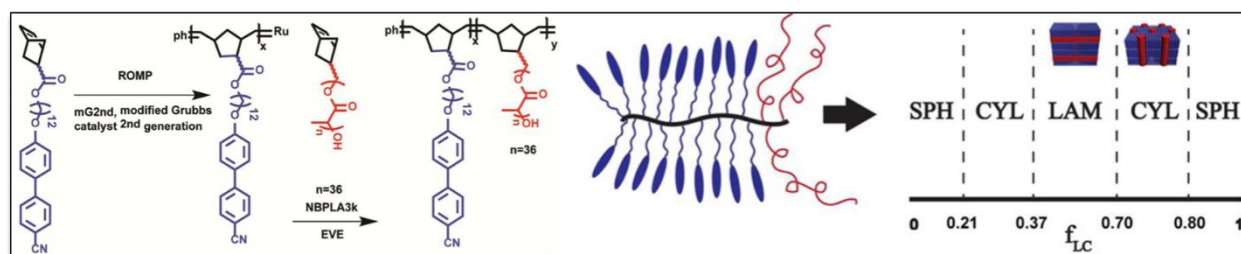


Figure 8: Synthesis and morphological behavior of liquid crystalline brush-like block copolymers. Long axes from PLA cylinders are parallel to SmA normal indicating planar anchoring. Reprinted with permission from Ref. 99. Copyright (2015) American Chemical Society.

Morphological studies indicate that LCBBCs display a phase behavior that is very similar to that observed in linear coil-coil diblock copolymers, Figure 8.⁹⁹ The domain spacing scales with molecular weight as $L_0 \sim MW^{0.6}$ representing a strong departure from the behavior of bottlebrush block copolymers where $L_0 \sim MW^1$.⁹⁹ The self-assembly of LCBBCs may be more analogous to side-chain LC diblock copolymers or graft-coil block copolymers than to that of bottlebrush block copolymers. The morphology of LCBBC may also depend on the mesogen anchoring condition at the IMDS during field directed self-assembly, Figure 8.^{35, 99}

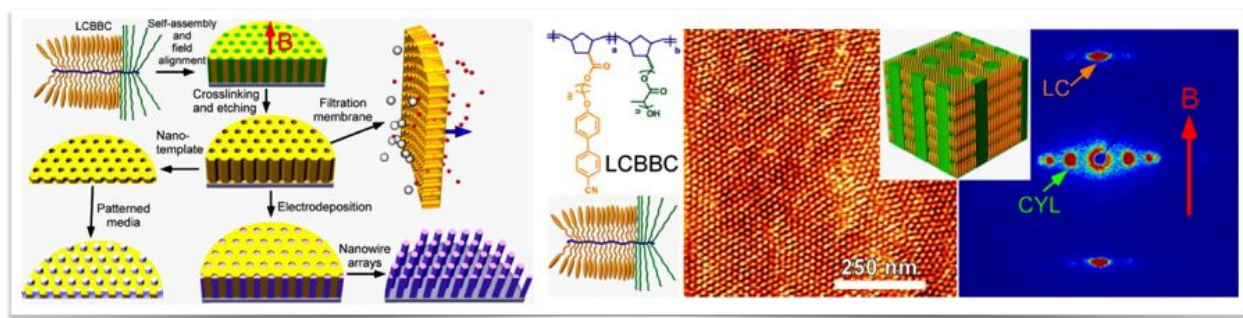


Figure 9: Nanoporous functional materials achieved by etching out PLA resulting in magnetically well aligned nanopores. The self-assembly of LCBBCs closely resembles that of LC diblock copolymers and graft-coil BCPs rather than bottlebrush BCPs. Adapted with permission from Ref 35. Copyright (2014) American Chemical Society.

Recent work on magnetic field directed assembly and selective etching of poly(DL-lactide) (PLA) microdomains in a PLA-containing brush-like LCBBCP has been exploited to create aligned nanopores in polymer film, Figures 9 and 10.^{26, 27, 35, 100} The system showed the ability to reversibly open and close the pores due to response to Laplace pressure induced pore collapse on softening at elevated temperatures.¹⁰⁰ Strategies to blend reactive and crosslinkable mesogens to decrease viscosity will help manipulate order-disorder transition temperature and self-assembly, reduce the magnetic field strength used, pattern and align mesophases for creation of new LC elastomer based adaptive materials.^{26, 27}

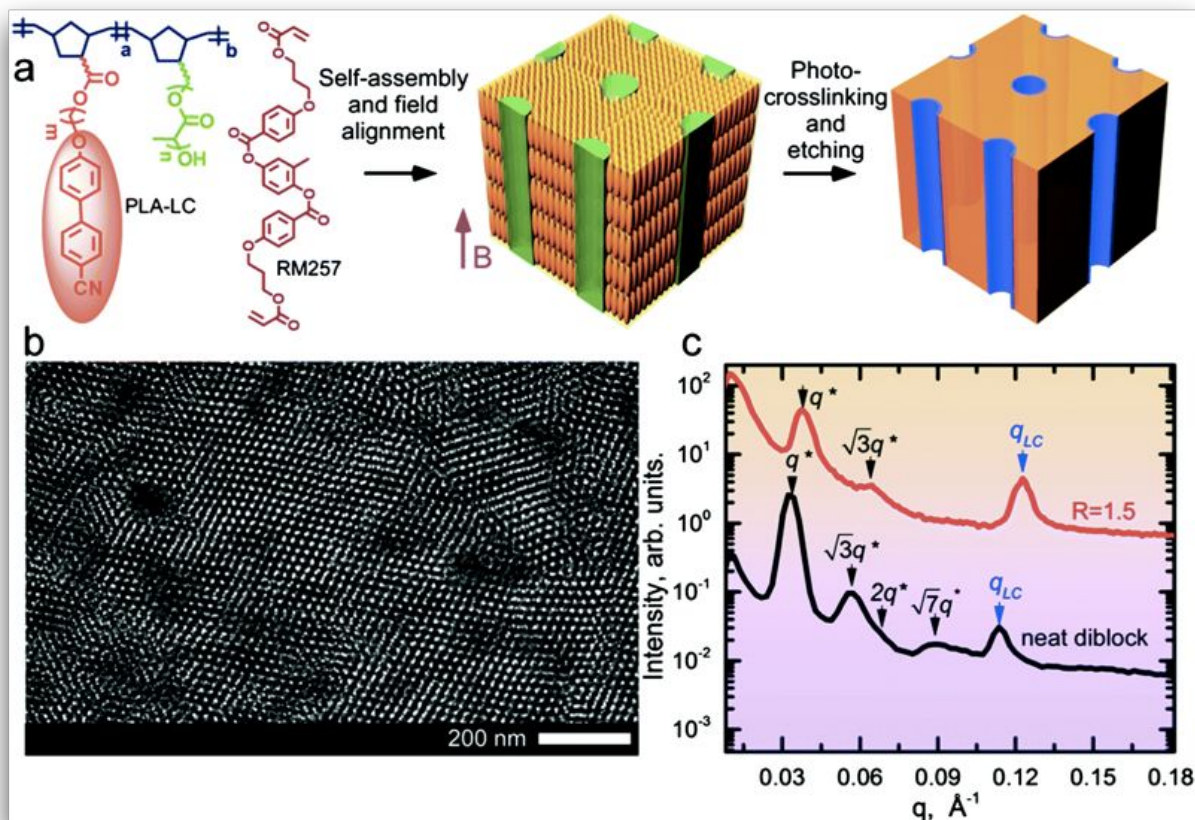


Figure 10: Liquid crystalline brush-like block copolymers are blended with reactive mesogens to decrease viscosity of the blends. This helps tune order-disorder temperature, aid self-assembly and ultimately reduce magnetic field strengths needed for alignment. Low magnetic fields are used in aligning LC domains as depicted by SAXS, followed by PLA etching and crosslinking leads to mechanically robust nanoporous films. Reproduced from Ref. 27 with permission from The Royal Society of Chemistry, Copyright (2017).

Section 3.2: Liquid crystalline block copolymers bearing organic dye molecules

The vast majority of LCBCPs bearing dyes reported in the literature involve azobenzene platforms, where the azobenzene moiety functions both as a dye as well as a LC mesogen.¹⁰¹ In one study, Tian and coworkers prepared novel well-defined azobenzene containing liquid crystalline homopolymers. They also synthesized LCBCPs bearing functional azobenzene units in one block and PEO in the other block by ATRP.¹⁰² The homopolymers show SmA, SmC and unknown SmX mesophases and the block copolymers show cylindrical and/or spherical morphologies due to the PEG contained in the LC block when annealed in the smectic phase.¹⁰² On using UV-vis spectroscopy to compare the photophysical and photochemical properties of the annealed homopolymers with annealed block copolymers, it is concluded that the difference in the results is based on the ability of the block copolymers to form nanostructures.¹⁰² Due to lack of the nanostructures in the homopolymers, the H aggregations of the azobenzene moiety is very strong leading to complex trans-cis photochemical processes.^{103, 104} The nanostructures formed in the block copolymers prevent the formation of H-aggregates resulting in easier photochemical

processes.¹⁰² This finding can potentially open new opportunities in the field of holography and optical storage that involves azobenzene based block copolymers.

In another example, azobenzene-functionalized siloxane oligomers are synthesized as block molecules that resemble the block copolymer-like behavior when undergoing telechelic supramolecular polymerization.¹⁰⁵ In this report, the hydrogen bonding that promotes supramolecular polymerization forbids the crystallization of azobenzene enabling columnar/complex morphologies.¹⁰⁵ This behavior is very different when compared to the case without supramolecular polymerization where optimum balance between the self-assembly and azobenzene crystallization causes lamellar to isotropic transformations due to isomerization under UV light accompanied by fast and reversible solid to liquid phase transitions.¹⁰⁶⁻¹⁰⁸ The mechanical properties coupled with their nanostructures make them suitable for photolithography and photo-switchable materials.¹⁰⁵

Section 4.0: Liquid crystalline statistically random copolymers from the copolymerization of conventional non-LC monomers and end-on attached side-chain liquid crystalline monomers

Copolymerization of non-LC monomers (acrylate, methacrylate, norbornene or lactone monomer) and LC monomers (acrylate, methacrylate, norbornene or lactone monomer) in a statistically random process by conventional free radical, ring opening and ring opening metathesis polymerization results liquid crystalline statistically random copolymers. These copolymers are typically coil-coil in nature and have side-chain non-LC moiety end-on side-chain liquid crystalline mesogen attachment.¹⁰⁹ Synthetic strategies have been employed to achieve a high degree of control over comonomer incorporation, composition, polymer chain architecture, and thereby, easy to tune copolymer properties. However, due to the statistical nature of random comonomer incorporation and lack of periodicity of the polymer chain, hierarchical self-assembly may be difficult to attain although mesophase formation and associated liquid crystalline phase properties are still feasible to retain.¹¹⁰

Many examples of liquid crystalline random copolymers comprising chiral side-chain LC units with or without crosslinks have been synthesized. These random copolymers and elastomers self-assemble to form the 1D photonic helical cholesteric (Ch*) or ferroelectric SmC* mesophase. These materials have been used to create photonic materials as well as actuators having shape morphing properties.^{46, 82, 86, 111-128} With Ch* mesophase, the selective light reflection of incoming light can be observed from the surface of the copolymer film when the result of the product of the helical pitch and average refractive index of a material falls under the wavelength of visible light. Additionally, the helical pitch can be altered by various methods like temperature, chiral dopants and application of electrical or mechanical fields. This provides a handle for tuning the optical properties of the polymeric materials and for designing tunable mirrorless lasers, electro-optical devices, color (or contrast) tuning/recording devices and holography.^{30, 43, 44, 129-132}

Section 4.1: Liquid crystalline random copolymers from the polymerization of novel branched non-LC monomers (macromonomers) and end-on side-chain liquid crystalline monomers

We discussed examples of LCBCPs incorporating both LC moieties and semicrystalline PEO-type block where there are three structure forming units: LC units, semicrystalline polymers and block copolymer architecture that compete resulting in a hierarchical self-assembled structure. In such systems, most research has been concentrated on the LCBCPs comprising linear semicrystalline polymers (e.g., poly(ethylene glycol), PEG) as the first block and LC units in the second block.²³ In these cases, LC order competes with crystallization of PEG domains within microphase segregated structures resulting mostly in cylindrical and lamellar domains.²⁴ The impact of semicrystalline PEG having branched architectures including graft, brush, or comb architectures on the self-assembly of LCBCPs has yet to be explored. Furthermore, hierarchical self-assembled structures with curvatures including spherical and helical structures need to be identified. The densely grafted brush, comb or graft type semicrystalline or amorphous non-LC polymers encompass reduced entanglements that exhibit unprecedented nanostructure formations with interesting mechanical and optical properties.¹³³⁻¹³⁵

Using ROMP, our group has been able to design different hierarchical architectures of polynorbornene based liquid crystalline random brush copolymers (LCRBC) consisting of (i) LC units including cholesteryl, cyanobiphenyl and/or azobenzene mesogens and (ii) non-LC PEG side chains, Figure 11.^{37, 47, 136, 137} This architecture provides an excellent platform to incorporate self-assembled nanostructures on multiple length scales: LC smectic mesophase order at 3–7 nm, microphase segregation of amorphous PEG side chain at 10–12 nm, and periodicity in cholesteric mesophase at scales greater than 100 nm, Figure 10.^{37, 47, 136, 137} This hierarchical structure formation is feasible only at weight fractions of PEG less than 25 wt% when PEG domains are amorphous in nature.^{37, 47, 136} Although helical multilevel hierarchical materials have been demonstrated using BCP polypeptides, to the best of our knowledge cholesteric phase in conjunction with microphase segregated domain has never been observed. The key to the observed hierarchical assembly lies in the interplay of LC order, PEG side chain microphase segregation into amorphous domains, and their supramolecular cooperative motion, which allow a controlled structure formation on each discrete length scale. Similar to self-assembly of some biological structures, this unique “single component” polymer scaffold transforms our capacity to attain nanoscale hierarchies resulting from the combination of LC, brush-like PEG side chain, and random copolymer architecture. However, these LC random copolymers present blue light visible reflections and are very brittle.⁴⁷

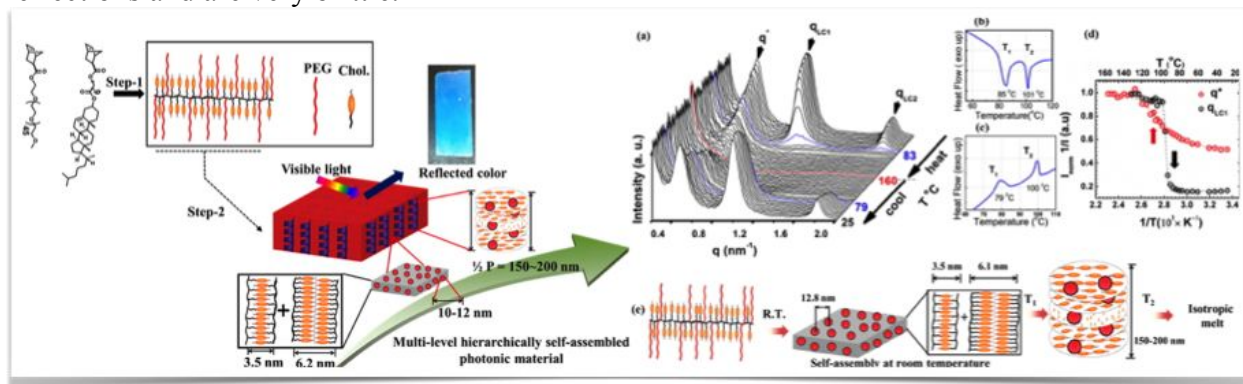


Figure 11: Nanoscale hierarchical structures from liquid crystalline brush-like random copolymers resulting in photonic band gap materials. These hierarchical structures result from the interplay

between microphase segregation of brush-like units and LC order. Adapted with permission from Ref. 47. Copyright (2013) American Chemical Society

To address these issues two subsequent studies were published. In one example, polynorbornene random terpolymers consisting of (i) two different side chain monomers bearing cholesterol and UV-responsive azobenzene and (ii) a side chain PEG monomer respectively have been synthesized to tune the reflection band to longer wavelengths (near IR region).³⁷ In the work published by Ndaya and Bosire, as shown in Figure 12, the terpolymers are compression molded at specific temperatures based on liquid crystalline thermal transitions to achieve cholesteric mesophase. Optical reflections can be tuned to longer wavelengths (825 nm) as a result of the LC-LC interactions by the introduction of azobenzene mesogen in the liquid crystalline polymer system.³⁷ These polymer films are brittle and to improve the mechanical properties, side chain polyethylene glycol bearing norbornene monomer are introduced in the copolymer systems to impart plasticizing effect to the polymeric films. To overcome this issue, polynorbornenes bearing two different LC units (cyano-biphenyl and cholesteryl mesogens) and PEG side chains were synthesized. The polynorbornene backbone is crosslinked by thiol-ene chemistry.¹³⁶ In this system, optimal elastomeric and shape memory features are attained in addition to blue/green light reflecting photonic materials.¹³⁶

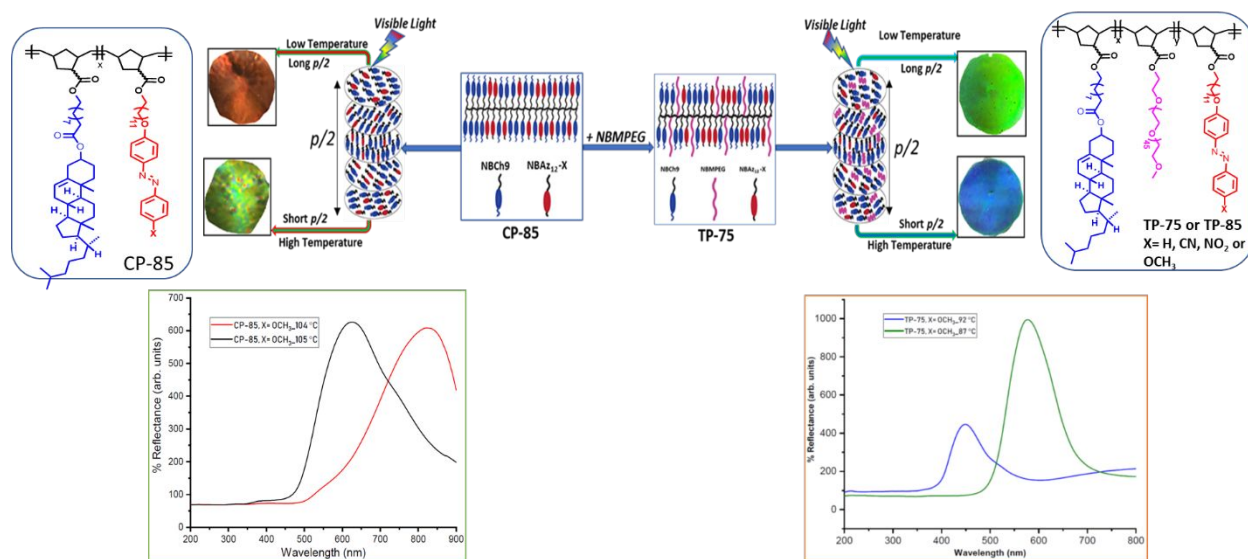


Figure 12: Azobenzene dye, cholesterol and polyethylene glycol units are covalently attached to norbornene backbone. In these copolymers and terpolymers, liquid crystalline–liquid crystalline (LC-LC) interactions between the LC mesogens cholesterol and azobenzene led to a wider range of colors reflected. An increase in temperature led to a hypsochromic shift while a decrease in temperature led to a bathochromic shift. The shift in reflections from near-IR to visible regions was reversible. Change in monomer composition or stimuli controlled the cholesteric mesophase helical pitch. Adapted with permission from Ref 37. Copyright (2019) Royal Society of Chemistry.

Thus, there is a need to develop LCPs that can change color on the application of both mechanical and thermal stimuli exhibiting reversible mechano-thermo-chromic features. Besides,

the reflection bandwidth in some of these materials is still very narrow (few tens of nm). Thus, the main aim is to broaden the reflection band of these existing materials and introduce a change in color upon both mechanical force and increment in temperature.

Section 4.2 Liquid crystalline random copolymers and networks bearing organic dye molecules

Hybrid materials comprising LC polymer framework and dye molecules new insights on how dyes significantly impact the optical, morphological, mechanical properties and applications of the liquid crystalline systems are obtained. For example, dye doped LCPs as well as dyes covalently bound with LC framework highly ordered and aligned polymeric materials that retain both the properties of the LCs even at high dye concentrations. These hybrid materials exhibit electro-optical effects that could be used for reversible optical information storage, optoelectronics and displays.¹³⁸⁻¹⁴⁰

Yue and coworkers reported crosslinked liquid crystalline polymers that contained a photo melting azobenzene monomer that not only acted as a crosslinker but also as a photoresponsive moiety. Free standing polymer films are prepared by free radical polymerization of azobenzene monomer along with DGI (non photoresponsive LC monomer). These polymer films showed reversible photo switchable glass transition temperature (T_g) along with reversible photomechanical response. The azobenzene monomer is photoresponsive exhibiting trans-cis isomerization on exposure to UV. The isomerization is accompanied by a phase change from solid (trans form) to liquid (cis form). Owing to this property the resulting liquid crystalline networks could tune the glass transition temperature on exposure to photo-radiation. The meta substituted methyl azobenzene monomer favored the solid-liquid phase change contrary to the H-substituted structure which did not show similar property suggesting that precise tailoring of the monomer played a significant role in imparting responsive properties to the polymer. The morphological studies indicated the existence of SmC mesophase with respect to the non photoresponsive LC monomer in the polymer film. Tensile tests on the polymer film concluded the Young's modulus to be high when existing in the trans form (higher T_g) and lower Young's modulus with higher percentage elongation when existing in the cis form (lower T_g). These results support the idea that molecular engineering is the tool to introduce and even intensify stimuli responsive properties into polymeric frameworks. Incorporating stimuli-responsive switches into highly ordered LC polymeric networks can enhance the overall molecular motion. Such examples provide deeper insights on the structure-property of the stimuli-responsive dyes and the impact they can have when coupled with LC monomers.¹⁰⁸

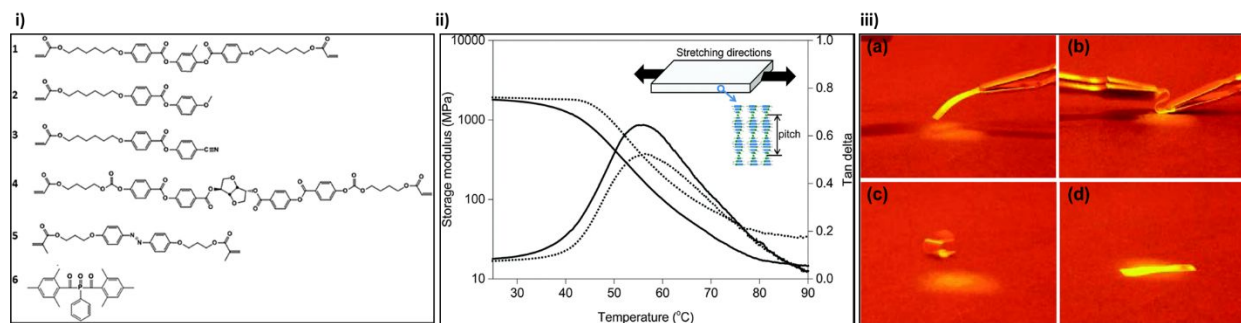


Figure 13: (i) Compounds (1- 6) are used to synthesize nematic cholesteric liquid crystalline network. (ii) Stretching direction with respect to liquid crystal alignment in polymerized films (inset). Storage modulus and tan delta as a function of temperature of two tested chiral-nematic polymer networks (bottom). The solid line relates to the liquid crystal network (LCN) with low crosslink density and the dashed line is the LCN with high crosslink density. (iii) Shape memory effect in LC polymer film: (a) before dual light treatment, (b) subjected to dual light illumination and deformed into a curled shape, (c) shape after the dual light treatment and (d) recovered the initial shape upon dual light exposure. Reproduced from Ref 123 with permission from The Royal Society of Chemistry, Copyright (2016).

Schenning, Broer and coworkers reported a unique approach to manipulate the elastic modulus of azobenzene containing liquid crystal networks (LCNs) by exposure to light, Figure 13.^{122, 123} The elastic modulus can cycle between different levels by controlling the illumination conditions. Exposing the polymer network to UV light near the trans isomer absorption band of azobenzene results in lower T_g thereby lowering the modulus.¹²³ The addition of blue light near the cis isomer absorption band surprisingly amplifies this effect.^{122, 124} A large shift of glass transition temperature and modulus decrease has been attributed to the chain dynamics of the LCNs. The initial high modulus and the glassy state were recovered quickly by switching off the light sources, despite the azobenzene being in the cis state.¹²² Based on these new findings, shape memory polymer LCNs film are designed to function room temperature using light, Figure 13.¹²³⁻¹²⁷

4.3 Incorporation of dyes within liquid crystalline networks and polymer stabilized liquid crystals for smart applications

Strategic design of smart windows in buildings is advantageous as they balance access to solar gains and thermal transmission. With the aim of developing materials that can tune optical properties on exposure to solar radiation, many researchers have tried to tune the reflection properties of cholesteric liquid crystals (CLCs).^{128, 141} As mentioned before, the self-organized molecular helices of the CLCs are responsible for their optical properties where the pitch of the helix determines the wavelength of reflection. The selective reflection bandwidth of the CLCs offers many advantages but is normally limited to 100-200 nm based on the central wavelength and birefringence.¹²⁸ To address the issue of energy consumption for smart window applications, responsive windows containing CLCs need to include a wider range of wavelengths by broadening the spectrum and red shifting their reflection band. In a recent example, a UV-responsive azobenzene chiral dye is incorporated into a cholesteric liquid crystalline network. Several compositions are prepared by mixing a nematic liquid crystal, a chiral dopant, a nematic LC monomer, a photoinitiator and an azobenzene chiral dopant with varying compositions.¹²⁸ It is filled into a cell consisting of two ITO glasses with a thickness of 20 μm and the cell is then irradiated by UV light.¹⁴² On exposure to UV light for 30 mins at 40 $^{\circ}\text{C}$, the UV dye absorbs UV light and creates a UV gradient throughout the cell allowing the crosslinking to occur mainly in the upper part of the cell which is exposed to UV.^{130, 142} As azobenzene dye is known to undergo trans-cis isomerization upon exposure to UV, the upper part of the cell is mostly converted to the cis-isomer whereas the lower part remains in the trans form. On switching the UV light with visible light (450 nm) for 20 mins, the cis form that possesses low helical twisting power (HTP) and which is present in the lightly crosslinked region goes back to the trans form (high HTP) but the cis form

present in the densely crosslinked domain is unable to convert back into the trans form. The coexistence of both cis (low HTP) and trans (high HTP) state of azobenzenes along the thickness of the film causes a pitch gradient from top to bottom broadening the reflection wavelength of the sample, which is about 1400 nm covering 1000–2400 nm as compared to 100–200 nm, Figure 14.^{128, 131, 132}

To broaden the cholesteric reflection band, a polymer network is used to create a broadband IR reflector comprising of a coumarin based fluorescent dye for generating electricity or an energy generating window.¹⁴³ In this study, 0.25 wt% of the coumarin dye that partially absorbed light in the visible region is added to the cholesteric liquid crystal mixture containing the photoinitiator and crosslinker followed by photopolymerization. On applying an electric voltage to the cell, the peak absorption of the dye decreased indicating that the dye is well aligned with the liquid crystal producing a homeotropic alignment.¹⁴³ On exposing the cell to sunlight, the dye absorbed light and emitted at longer wavelengths along with a portion of light undergoing total internal reflection that could be converted into electrical current by connecting a photovoltaic cell at the edge of the glass plate.¹⁴³

Recently, polymer stabilized liquid crystals (PSLC) gained attention as potential candidates for fabricating smart windows. An azobenzene side chain liquid crystalline copolymer (MAzo-co-GMA) synthesized through copolymerizing the monomer 6-(4-((4-butylphenyl)-diazanyl)phenoxy)hexyl methacrylate (MAzo) with glycidylmethacrylate (GMA) by ATRP proved to be a successful candidate in forming stable polymer brush on a substrate and inducing photothermal effect. This copolymer solution is spin-coated on glass substrates followed by thermal crosslinking which allowed the epoxy groups to crosslink with the hydroxy groups on the glass surface. A chiral LC mixture containing nematic LCs, photoinitiator Irgacure 784, a chiral dopant, and photopolymerizable monomer is heated to an isotropic phase and sandwiched in between the copolymer coated glass substrates. The LCs existed in SmA* phase upon cooling, and on exposure to white light the photopolymerizable monomer induced crosslinking ultimately forming PSLC. The PSLC showed a transparent state due to the homeotropic alignment imparted by the stable polymer brush in the SmA* phase. However, on exposure to UV light or heat, the azobenzene incorporated within the copolymer brush induced a photothermal effect that led to a phase transition from a transparent (SmA*) to opaque state (N*). It is observed that the responsive behavior of the PSLC relied on concentration of the copolymer brush and intensity of the UV light. The stability and good reversibility of this effect made this PSLC system a suitable candidate for energy saving devices. This example highlights the importance of a stimuli-responsive azobenzene dye that serves as a driving force for the LC phase change necessary for the fabrication of a smart window.¹⁴¹

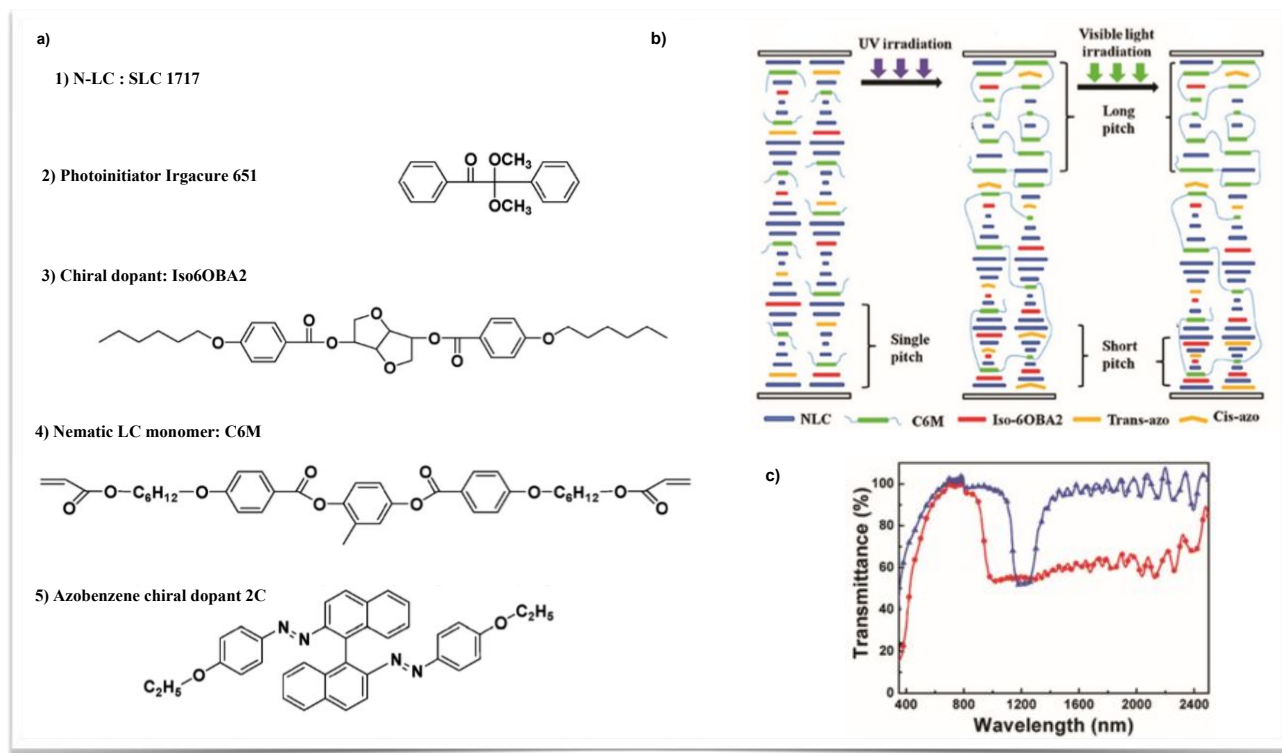


Figure 14: a) (1-5) Components used to prepare the composite b) Schematic illustration to demonstrate the mechanism of broadband reflector doped with chiral azobenzene in CLC network. c) Transmission spectrum of CLC film indicating the broadening of the band. Initial (blue) and after exposing to UV-light (red). Reproduced from Ref. 128 with permission from The Royal Society of Chemistry, Copyright (2014).

Lasing is another interesting application of dye incorporated cholesteric liquid crystalline materials. Laser dyes have been physically doped within liquid crystalline polymers to combine optical (luminescent or fluorescent) properties of the dyes with optical anisotropic properties of the liquid crystalline polymers.^{131, 144, 145} A classical demonstration of this idea is the physical incorporation of fluorescent 4-(dicyanomethylene)-2-methyl-6-(4-dimethylaminostyryl)-4-Hpyran (DCM) dye doped within cholesteric liquid monodomain elastomers for tunable mirrorless lasing.¹⁴⁴ Finkelmann and coworkers have shown that the fluorescence emission of the dye is used along with the selective reflection band of the cholesteric liquid crystal monodomains to produce sharp and narrow lasing signals.⁴³ Cholesteric liquid crystal acts as distributing cavity and its bandgap structure favors lasing without the need of external mirrors. One of the normal modes of the emitted light is obstructed when the fluorescence emission of a fluorescent dye falls into the selective reflection wavelength region of the helical cholesteric structure. As a result, the modified fluorescence emission lowered its emission in the reflection band and intensified its emission along the band edge giving rise to sharp lasing signals. Finkelmann, Palffy-Muhoray and coworkers showed that the lasing features could be tuned by mechanical strain due to the optically responsive nature of the cholesteric phase to mechanical strain.^{43, 144, 146}

These were some of the examples where dyes could extend the applications of the liquid crystalline materials but there are still many more to be explored. There is a need to develop LCPs that can change color on the application of both mechanical and thermal stimuli exhibiting

reversible mechano-thermo-chromic features. Such materials can be well suited for mechanical damage sensing, thermal sensing, lasing and actuators.

4.4. Chemical attachment

Dichroic dyes have been covalently attached to polymer backbone, which can be aligned into uniaxially oriented films. Despite high dye concentrations, both the LC features and the optical features of the dye molecules are retained. These films exhibit electro-optical effects that could be used for reversible optical information storage, optoelectronics and displays have been reported by incorporation of dichroic dyes along with liquid crystalline polymers.¹³⁸⁻¹⁴⁰ For example, many azobenzene LCPs have been developed for photonic and photomechanical actuation applications.⁸³ For example, in a recent study from our research group, statistically random copolymers containing side chain azobenzene LC dye and side chain LC cholesteryl moiety are synthesized, Figure 12.³⁷ Statistical copolymers of these two side chain monomers, one bearing cholesterol and the other UV-responsive azobenzene self-assemble into cholesteric mesophase. Using the push-pull effects of different functionalities on azobenzene LC moiety as well as the composition of the copolymer, the reflection band can be tuned from visible to near IR wavelengths. This study proves that the optical reflections of these materials could be tuned as a result of the LC-LC interactions by the introduction of azobenzene mesogen in the liquid crystalline polymer (LCP) system.³⁷

5.0 Outlook on molecularly engineered, stimuli responsive, liquid crystalline polymers

The field of molecular engineered side-chain LCPs is focused on the impact of the polymer architecture and choice of specific LC and non-LC moieties to influence overall self-assembly and mesophase controlled thermo-mechano-optical properties. Homo- and copolymerization of side-chain LC monomers with other LC or non-LC monomers is one of the synthetic methods used to tailor the mesophase transitions of side-chain liquid crystalline polymers.⁶⁴ For example, homo- and copolymerization of chiral LC monomers results in cholesteric mesophases, which show 1D photonic properties.¹⁴⁷ However other chiral LCPs present frustrated phases, including blue phases and twisted grain boundary phases, result SmC* mesophase with selective reflection changes to the photonic band gap or fast switching electro-optical behavior.¹⁴⁸ These LCPs are used in actuators, optical materials, optoelectronics, photonics, holography, display technology, telecommunications systems, and ferroelectric applications.

The design of LCPs which respond to chemicals, heat, light, pressure, electricity or magnetic field is being embraced. For example, dye bearing LCs for piezochromic features are currently being explored. These materials rely on chromophores that display pronounced fluorescence and/or absorption color changes upon self-assembly as a result of charge-transfer interactions and/or conformational changes alongside interactions emanating from polymer architecture, sequence and choice of blocks with specific features.¹⁴⁹

New strategies of manipulating interfaces at the molecular level with random and block architectures are also being explored. Molecular interactions are expected to enhance the formation of unique hierarchically ordered structures similar to cooperative LC-LC interactions. For example, interactions between different mesophases such as SmA-SmC, SmA-SmC* or SmA-

cholesteric mesophases results in diverse features such as photonic, ferro- and piezoelectricity.¹⁴⁸ Inclusion of ligand appending functionalities within these new LCP architectures enable removal of heavy metals in filtration applications, catalysis and opportunities to couple LC properties with that of nanoparticles that tether to the ligands.^{25, 45, 150} Finally using new LCP architectures in conjunction with processing, aligning and orienting capabilities results in highly ordered functional soft templates for lithographic applications.²⁶

Finally, there is a trend towards the synthesis, properties and applications of LC materials derived from sustainable resources that will also degrade after use while retaining advantageous properties of synthetic LC materials.¹⁵¹ Use of sustainable and renewable macromolecules such as carbohydrates, polypeptides and proteins conjugated or blended with synthetic or naturally occurring LCs to create new stimuli responsive, functional, sustainable and degradable liquid crystalline materials will be an important area of research.

Acknowledgements

This work is supported by the National Science Foundation under DMR-1507045 and under CMMI-1246804. The central instrumentation facilities at the Institute of Materials Science and Chemistry Department at UConn are acknowledged. The authors thank Dr. Prashant Deshmukh, Dr. Lalit Mahajan, Prof. Chinedum Osuji, Dr. Manesh Gopinadhan and Dr. Youngwoo Choo for useful discussions. The authors also thank the reviewers and the editor of this manuscript for their insightful comments, which has been very helpful in revising this manuscript.

Conflicts of interest

There are no conflicts of interest to declare.

References:

1. G. Mao and C. K. Ober, *Acta Polymerica*, 1997, **48**, 405-422.
2. C. Tschierske, *Angew. Chem., Int. Ed.*, 2013, **52**, 8828-8878.
3. H. Yu, T. Kobayashi and H. Yang, *Advanced Materials*, 2011, **23**, 3337-3344.
4. J. Ping, K. Gu, S. Zhou, H. Pan, Z. Shen and X.-H. Fan, *Macromolecules*, 2016, **49**, 5993-6000.
5. L.-Y. Shi, J. Lan, S. Lee, L.-C. Cheng, K. G. Yager and C. A. Ross, *ACS Nano*, 2020, **14**, 4289-4297.
6. M. Walther and H. Finkelmann, *Progress in Polymer Science*, 1996, **21**, 951-979.
7. V. Abetz and P. F. W. Simon, *Phase behaviour and morphologies of block copolymers, In Block Copolymers I*, 2005.
8. S. Park, Y. Kim, H. Ahn, J. H. Kim, P. J. Yoo and D. Y. Ryu, *Scientific Reports*, 2016, **6**, 36326.
9. H.-Y. Hsueh, C.-T. Yao and R.-M. Ho, *Chemical Society Reviews*, 2015, **44**, 1974-2018.
10. G. Jeong, D. M. Yu, J. K. D. Mapas, Z. Sun, J. Rzayev and T. P. Russell, *Macromolecules*, 2017, **50**, 7148-7154.
11. H. Feng, X. Lu, W. Wang, N.-G. Kang and J. W. Mays, *Polymers*, 2017, **9**, 494.

12. J. Cortese, C. Soulié-Ziakovic, M. Cloitre, S. Tencé-Girault and L. Leibler, *Journal of the American Chemical Society*, 2011, **133**, 19672-19675.
13. W. Wang, X. Wang, F. Jiang and Z. Wang, *Polymer Chemistry*, 2018, **9**, 3067-3079.
14. Y. Guan, X. Chen, H. Ma, Z. Shen and X. Wan, *Soft Matter*, 2010, **6**, 922-927.
15. E. Verploegen, T. Zhang, Y. S. Jung, C. Ross and P. T. Hammond, *Nano Lett*, 2008, **8**, 3434-3440.
16. C. O. Osuji, J. T. Chen, G. Mao, C. K. Ober and E. L. Thomas, *Polymer*, 2000, **41**, 8897-8907.
17. Y. Zhou, S.-k. Ahn, P. Deshmukh and R. M. Kasi, *Liquid Crystalline Block Copolymers, In Encyclopedia of Polymer Science and Technology, (Ed.)*, 2013.
18. X.-F. Chen, Z. Shen, X.-H. Wan, X.-H. Fan, E.-Q. Chen, Y. Ma and Q.-F. Zhou, *Chemical Society Reviews*, 2010, **39**, 3072-3101.
19. R. Abeyssekera, R. J. Bushby, C. Caillet, I. W. Hamley, O. R. Lozman, Z. Lu and A. W. Robards, *Macromolecules*, 2003, **36**, 1526-1533.
20. H. Yang, L. Jia, C. Zhu, A. Di-Cicco, D. Levy, P.-A. Albouy, M.-H. Li and P. Keller, *Macromolecules* 2010, **43**, 10442-10451.
21. H. Komiyama, R. Sakai, S. Hadano, S. Asaoka, K. Kamata, T. Iyoda, M. Komura, T. Yamada and H. Yoshida, *Macromolecules*, 2014, **47**, 1777-1782.
22. W.-N. He and J.-T. Xu, *Progress in Polymer Science*, 2012, **37**, 1350-1400.
23. Y. Zhou, S.-k. Ahn, R. K. Lakhman, M. Gopinadhan, C. O. Osuji and R. M. Kasi, *Macromolecules*, 2011, **44**, 3924-3934.
24. P. Deshmukh, S.-k. Ahn, L. Geelhand de Merxem and R. M. Kasi, *Macromolecules*, 2013, **46**, 8245-8252.
25. C. T. Nguyen and R. M. Kasi, *Chem Commun*, 2015, **51**, 12174-12177.
26. M. Gopinadhan, Y. Choo, K. Kawabata, G. Kaufman, X. Feng, X. Di, Y. Rokhlenko, L. H. Mahajan, D. Ndaya, R. M. Kasi and C. O. Osuji, *Proceedings of the National Academy of Sciences*, 2017, **114**, E9437.
27. M. Gopinadhan, Y. Choo, L. H. Mahajan, D. Ndaya, G. Kaufman, Y. Rokhlenko, R. M. Kasi and C. O. Osuji, *Molecular Systems Design & Engineering*, 2017, **2**, 549-559.
28. Y. Rokhlenko, M. Gopinadhan, C. O. Osuji, K. Zhang, C. S. O'Hern, S. R. Larson, P. Gopalan, P. W. Majewski and K. G. Yager, *Phys Rev Lett*, 2015, **115**, 258302.
29. H.-L. Xie, X. Li, J. Ren, C. Bishop, C. G. Arges and P. F. Nealey, *Journal of Polymer Science Part B: Polymer Physics*, 2017, **55**, 532-541.
30. N. Tamaoki, *Advanced Materials*, 2001, **13**, 1135-1147.
31. Y. Zhou, V. A. Briand, N. Sharma, S.-k. Ahn and R. M. Kasi, *Materials*, 2009, **2**, 636-660.
32. Y. Zhou and R. M. Kasi, *Journal of Polymer Science, Part A: Polymer Chemistry*, 2008, **46**, 6801-6809.
33. E. Verploegen, T. Zhang, N. Murlo and P. T. Hammond, *Soft Matter*, 2008, **4**, 1279-1287.
34. S. K. Ahn, L. T. Nguyen Le and R. M. Kasi, *Journal of Polymer Science Part A: Polymer Chemistry*, 2009, **47**, 2690-2701.
35. P. Deshmukh, M. Gopinadhan, Y. Choo, S.-k. Ahn, P. W. Majewski, S. Y. Yoon, O. Bakajin, M. Elimelech, C. O. Osuji and R. M. Kasi, *ACS Macro Letters*, 2014, **3**, 462-466.
36. D. A. Paterson, A. Martínez-Felipe, S. M. Jansze, A. Tm Marcelis, J. Md Storey and C. T. Imrie, *Liquid Crystals*, 2015, **42**, 928-939.
37. D. Ndaya, R. Bosire and R. M. Kasi, *Polymer Chemistry*, 2019, **10**, 3868-3878.

38. G. Mao, J. Wang, S. R. Clingman, C. K. Ober, J. T. Chen and E. L. Thomas, *Macromolecules*, 1997, **30**, 2556-2567.
39. M. Wang, W.-W. Bao, W.-Y. Chang, X.-M. Chen, B.-P. Lin, H. Yang and E.-Q. Chen, *Macromolecules*, 2019, **52**, 5791-5800.
40. X. Li and H. Yu, *Photoresponsive Liquid Crystalline Polymers*, Springer Berlin, Heidelberg, 2019.
41. V. Shibaev, *Liquid Crystalline Polymers, In Reference Module in Materials Science and Materials Engineering*, Elsevier, 2016.
42. S. Petsch, R. Rix, B. Khatri, S. Schuhladen, P. Müller, R. Zentel and H. Zappe, *Sensors and Actuators A: Physical*, 2015, **231**, 44-51.
43. H. Finkelmann, S. T. Kim, A. Muñoz, P. Palffy-Muhoray and B. Taheri, *Advanced Materials*, 2001, **13**, 1069-1072.
44. A. C. Edrington, A. M. Urbas, P. DeRege, C. X. Chen, T. M. Swager, N. Hadjichristidis, M. Xenidou, L. J. Fetters, J. D. Joannopoulos, Y. Fink and E. L. Thomas, *Advanced Materials*, 2001, **13**, 421-425.
45. D. Ndaya, R. Bosire, L. Mahajan, S. Huh and R. Kasi, *Polymer Chemistry*, 2018, **9**, 1404-1411.
46. S.-k. Ahn, M. Gopinadhan, P. Deshmukh, R. K. Lakhman, C. O. Osuji and R. M. Kasi, *Soft Matter*, 2012, **8**, 3185-3191.
47. P. Deshmukh, S.-k. Ahn, M. Gopinadhan, C. O. Osuji and R. M. Kasi, *Macromolecules*, 2013, **46**, 4558-4566.
48. L. Zhang, W. Yao, Y. Gao, C. Zhang and H. Yang, *Polymers*, 2018, **10**, 794.
49. T. Ganicz and W. Stańczyk, *Materials*, 2009, **2**, 95-128.
50. F. Liao, L.-Y. Shi, L.-C. Cheng, S. Lee, R. Ran, K. G. Yager and C. A. Ross, *Nanoscale*, 2019, **11**, 285-293.
51. H. Pan, W. Zhang, A. Xiao, X. Lyu, Z. Shen and X. Fan, *Macromolecules*, 2018, **51**, 5676-5684.
52. Y. Zhou, N. Sharma, P. Deshmukh, R. K. Lakhman, M. Jain and R. M. Kasi, *Journal of the American Chemical Society*, 2012, **134**, 1630-1641.
53. K. K. Tenneti, X. Chen, Q. Pan and C. Y. Li, *Structure and Assembly of Liquid Crystalline Block Copolymers, In Polymers and Polymeric Composites: A Reference Series*, Springer Berlin, Heidelberg, 2018.
54. T. Itoh, N. Tomikawa, M. Yamada, M. Tokita, A. Hirao and J. Watanabe, *Polymer Journal*, 2001, **33**, 783-791.
55. I. A. Ansari, V. Castelletto, T. Mykhaylyk, I. W. Hamley, Z. B. Lu, T. Itoh and C. T. Imrie, *Macromolecules*, 2003, **36**, 8898-8901.
56. L. Sun, J. E. Ginorio, L. Zhu, I. Sics, L. Rong and B. S. Hsiao, *Macromolecules*, 2006, **39**, 8203-8206.
57. L. Cui, J. Miao, L. Zhu, I. Sics and B. S. Hsiao, *Macromolecules*, 2005, **38**, 3386-3394.
58. T.-M. Chung, R.-M. Ho, J.-C. Kuo, J.-C. Tsai, B. S. Hsiao and I. Sics, *Macromolecules*, 2006, **39**, 2739-2742.
59. K. K. Tenneti, X. Chen, C. Y. Li, Y. Tu, X. Wan, Q.-F. Zhou, I. Sics and B. S. Hsiao, *Journal of the American Chemical Society*, 2005, **127**, 15481-15490.
60. L.-Y. Shi, Y. Zhou, X.-H. Fan and Z. Shen, *Macromolecules*, 2013, **46**, 5308-5316.
61. L.-Y. Shi, S. Lee, L.-C. Cheng, H. Huang, F. Liao, R. Ran, K. G. Yager and C. A. Ross, *Macromolecules*, 2019, **52**, 679-689.

62. S. Nagano, *Langmuir*, 2019, **35**, 5673-5683.
63. Y. Chen, S. Huang, T. Wang, Z. Dong and H. Yu, *Macromolecules*, 2019, **52**, 1892-1898.
64. R. Imanishi, Y. Nagashima, K. Takishima, M. Hara, S. Nagano and T. Seki, *Macromolecules*, 2020, **53**, 1942-1949.
65. X. Li, F. Huang, T. Jiang, X. He, S. Lin and J. Lin, *RSC Advances*, 2015, **5**, 1514-1521.
66. C. Park, J. Yoon and E. L. Thomas, *Polymer*, 2003, **44**, 6725-6760.
67. A. J. Soininen, I. Tanionou, N. ten Brummelhuis, H. Schlaad, N. Hadjichristidis, O. Ikkala, J. Raula, R. Mezzenga and J. Ruokolainen, *Macromolecules*, 2012, **45**, 7091-7097.
68. C. Osuji, P. J. Ferreira, G. Mao, C. K. Ober, J. B. Vander Sande and E. L. Thomas, *Macromolecules*, 2004, **37**, 9903-9908.
69. M. Anthamatten and P. T. Hammond, *Journal of Polymer Science Part B: Polymer Physics*, 2001, **39**, 2671-2691.
70. N. Tomikawa, Z. Lu, T. Itoh, C. T. Imrie, M.-a. Adachi, M. Tokita and J. Watanabe, *Japanese Journal of Applied Physics*, 2005, **44**, L711-L714.
71. J. P. Abberley, R. Killah, R. Walker, J. M. D. Storey, C. T. Imrie, M. Salamończyk, C. Zhu, E. Gorecka and D. Pocięcha, *Nature Communications*, 2018, **9**, 228.
72. C. Tschierske, *Israel Journal of Chemistry*, 2012, **52**, 935-959.
73. A. Gainar, M.-C. Tzeng, B. Heinrich, B. Donnio and D. W. Bruce, *The Journal of Physical Chemistry B*, 2017, **121**, 8817-8828.
74. A. Bubnov, M. Kašpar, V. Hamplová, U. Dawin and F. Giesselmann, *Beilstein Journal of Organic Chemistry*, 2013, **9**, 425-436.
75. H. Yu, *Progress in Polymer Science*, 2014, **39**, 781-815.
76. T. Ikeda, J.-i. Mamiya and Y. Yu, *Angewandte Chemie International Edition*, 2007, **46**, 506-528.
77. T. Ube and T. Ikeda, *Advanced Optical Materials*, 2019, **7**, 1900380.
78. S. Kim, T. Ogata and S. Kurihara, *Polymer Journal*, 2017, **49**, 407-412.
79. A. Emoto, E. Uchida and T. Fukuda, *Polymers*, 2012, **4**, 150-186.
80. H. Yu, Y. Naka, A. Shishido and T. Ikeda, *Macromolecules*, 2008, **41**, 7959-7966.
81. A. S. Matharu, S. Jeeva and P. S. Ramanujam, *Chemical Society Reviews*, 2007, **36**, 1868-1880.
82. S.-k. Ahn, T. H. Ware, K. M. Lee, V. P. Tondiglia and T. J. White, *Advanced Functional Materials*, 2016, **26**, 5819-5826.
83. Y. Zhao and J. He, *Soft Matter*, 2009, **5**, 2686-2693.
84. H. Yu, T. Iyoda and T. Ikeda, *Journal of the American Chemical Society*, 2006, **128**, 11010-11011.
85. H. Yu and T. Kobayashi, *Molecules*, 2010, **15**, 570-603.
86. T. Ube, K. Kawasaki and T. Ikeda, *Advanced Materials*, 2016, **28**, 8212-8217.
87. V. Castelletto, P. Parras, I. W. Hamley, P. Davidson, J. Yang, P. Keller and M.-H. Li, *Macromolecules*, 2005, **38**, 10736-10742.
88. D. Broer, G. P. Crawford and S. Zumer, *Cross-linked liquid crystalline systems: from rigid polymer networks to elastomers*, Boca Raton: CRC press, 2011.
89. M.-H. Li and P. Keller, *Philosophical Transactions: Mathematical, Physical and Engineering Sciences*, 2006, **364**, 2763-2777.
90. G. K. Sethi, X. Jiang, R. Chakraborty, W. S. Loo, I. Villaluenga and N. P. Balsara, *ACS Macro Letters*, 2018, **7**, 1056-1061.

91. X. Li, S. Cheng, Y. Zheng and C. Y. Li, *Molecular Systems Design & Engineering*, 2019, **4**, 793-803.
92. M. Gopinadhan, P. W. Majewski and C. O. Osuji, *Macromolecules* 2010, **43**, 3286-3293.
93. J. Li, K. Kamata, M. Komura, T. Yamada, H. Yoshida and T. Iyoda, *Macromolecules*, 2007, **40**, 8125-8128.
94. P. W. Majewski, M. Gopinadhan and C. O. Osuji, *Polymers* 2019, **11**, 887.
95. P. W. Majewski, M. Gopinadhan and C. O. Osuji, *Soft Matter*, 2013, **9**, 7106-7116.
96. P. W. Majewski, M. Gopinadhan, W.-S. Jang, J. L. Lutkenhaus and C. O. Osuji, *Journal of the American Chemical Society*, 2010, **132**, 17516-17522.
97. P. W. Majewski, M. Gopinadhan and C. O. Osuji, *Journal of Polymer Science Part B: Polymer Physics*, 2012, **50**, 2-8.
98. A. H. Gröschel and A. H. E. Müller, *Nanoscale*, 2015, **7**, 11841-11876.
99. Y. Choo, L. H. Mahajan, M. Gopinadhan, D. Ndaya, P. Deshmukh, R. M. Kasi and C. O. Osuji, *Macromolecules*, 2015, **48**, 8315-8322.
100. M. Gopinadhan, P. Deshmukh, Y. Choo, P. W. Majewski, O. Bakajin, M. Elimelech, R. M. Kasi and C. O. Osuji, *Advanced Materials*, 2014, **26**, 5148-5154.
101. L. Cui, Y. Zhao, A. Yavrian and T. Galstian, *Macromolecules*, 2003, **36**, 8246-8252.
102. Y. Tian, K. Watanabe, X. Kong, J. Abe and T. Iyoda, *Macromolecules*, 2002, **35**, 3739-3747.
103. M. E. Moustafa, M. S. McCreedy and R. J. Puddephatt, *Organometallics*, 2012, **31**, 6262-6269.
104. H. M. D. Bandara and S. C. Burdette, *Chemical Society Reviews*, 2012, **41**, 1809-1825.
105. R. H. Zha, G. Vantomme, J. A. Berrocal, R. Gosens, B. de Waal, S. Meskers and E. W. Meijer, *Advanced Functional Materials*, 2018, **28**, 1703952.
106. S. Guo, K. Matsukawa, T. Miyata, T. Okubo, K. Kuroda and A. Shimojima, *Journal of the American Chemical Society*, 2015, **137**, 15434-15440.
107. S. Peng, Q. Guo, T. C. Hughes and P. G. Hartley, *Langmuir*, 2014, **30**, 866-872.
108. Y. Yue, Y. Norikane, R. Azumi and E. Koyama, *Nature communications*, 2018, **9**, 3234-3234.
109. H. S. Nalwa, *Advanced functional molecules and polymers: electronic and photonic properties*, CRC Press, 2001.
110. J. Watanabe and W. Krigbaum, *Macromolecules*, 1984, **17**, 2288-2295.
111. H. Finkelmann and G. Rehage, *Liquid crystal side chain polymers*, In *Liquid Crystal Polymers II/III*, Springer Berlin, Heidelberg, 1984.
112. G. W. Gray, *Thermotropic liquid crystals*, John Wiley & Sons Inc, 1987.
113. J. Küpfer and H. Finkelmann, *Die Makromolekulare Chemie, Rapid Communications*, 1991, **12**, 717-726.
114. H. Finkelmann, H.-J. Kock and G. Rehage, *Die Makromolekulare Chemie, Rapid Communications*, 1981, **2**, 317-322.
115. J. Schätzle and H. Finkelmann, *Molecular Crystals and Liquid Crystals*, 1987, **142**, 85-100.
116. J. Küpfer and H. Finkelmann, *Macromolecular Chemistry and Physics*, 1994, **195**, 1353-1367.
117. L. T. de Haan, J. M. N. Verjans, D. J. Broer, C. W. M. Bastiaansen and A. P. H. J. Schenning, *Journal of the American Chemical Society*, 2014, **136**, 10585-10588.

118. L. T. de Haan, C. Sánchez-Somolinos, C. M. W. Bastiaansen, A. P. H. J. Schenning and D. J. Broer, *Angewandte Chemie International Edition*, 2012, **51**, 12469-12472.
119. A. J. J. Kragt, D. J. Broer and A. P. H. J. Schenning, *Advanced Functional Materials*, 2018, **28**, 1704756.
120. I. A. Rousseau and P. T. Mather, *Journal of the American Chemical Society*, 2003, **125**, 15300-15301.
121. W. Liu, L.-X. Guo, B.-P. Lin, X.-Q. Zhang, Y. Sun and H. Yang, *Macromolecules*, 2016, **49**, 4023-4030.
122. L. T. de Haan, A. P. Schenning and D. J. Broer, *Polymer*, 2014, **55**, 5885-5896.
123. K. Kumar, A. P. Schenning, D. J. Broer and D. Liu, *Soft Matter*, 2016, **12**, 3196-3201.
124. D. Liu, C. W. Bastiaansen, J. M. den Toonder and D. J. Broer, *Macromolecules*, 2012, **45**, 8005-8012.
125. D. Iqbal and M. H. Samiullah, *Materials*, 2013, **6**, 116-142.
126. Y. Li, Y. Zhang, M. Goswami, D. Vincent, L. Wang, T. Liu, K. Li, J. K. Keum, Z. Gao and S. Ozcan, *Soft Matter*, 2020, **16**, 1760-1770.
127. J. Yang, W. Zhao, Z. Yang, W. He, J. Wang, T. Ikeda and L. Jiang, *ACS Applied Materials & Interfaces*, 2019, **11**, 46124-46131.
128. X. Chen, L. Wang, Y. Chen, C. Li, G. Hou, X. Liu, X. Zhang, W. He and H. Yang, *Chemical Communications*, 2014, **50**, 691-694.
129. Y. J. Liu and X. W. Sun, *Advances in OptoElectronics*, 2008, **2008**, 684349.
130. A. Ranjakesh and T.-H. Yoon, *Journal of Materials Chemistry C*, 2018, **6**, 12377-12385.
131. H. Khandelwal, A. P. Schenning and M. G. Debije, *Advanced Energy Materials*, 2017, **7**, 1602209.
132. F. Wang, K. Li, P. Song, X. Wu, H. Chen and H. Cao, *Composites Part B: Engineering*, 2013, **46**, 145-150.
133. C. Tang, B. Dufour, T. Kowalewski and K. Matyjaszewski, *Macromolecules*, 2007, **40**, 6199-6205.
134. R. Verduzco, X. Li, S. L. Pesek and G. E. Stein, *Chem Soc Rev*, 2015, **44**, 2405-2420.
135. J. C. Foster, S. Varlas, B. Couturaud, Z. Coe and R. K. O'Reilly, *J Am Chem Soc*, 2019, **141**, 2742-2753.
136. L. H. Mahajan, D. Ndaya, P. Deshmukh, X. Peng, M. Gopinadhan, C. O. Osuji and R. M. Kasi, *Macromolecules*, 2017, **50**, 5929-5939.
137. L. Mahajan, D. Ndaya, P. Deshmukh, S.-k. Ahn and R. Kasi, *Elsevier*, 2017, **9**, 321-327.
138. R. R. Deshmukh and A. Katariya Jain, *Liquid Crystals*, 2014, **41**, 960-975.
139. P. Malik and K. K. Raina, *Physica B: Condensed Matter*, 2010, **405**, 161-166.
140. H.-W. Schinidt, *Advanced Materials*, 1989, **1**, 218-224.
141. Z.-Y. Kuang, Y. Deng, J. Hu, L. Tao, P. Wang, J. Chen and H.-L. Xie, *ACS Applied Materials & Interfaces*, 2019, **11**, 37026-37034.
142. A. Ryabchun and A. Bobrovsky, *Advanced Optical Materials*, 2018, **6**, 1800335.
143. H. Khandelwal, R. C. Loonen, J. L. Hensen, M. G. Debije and A. P. Schenning, *Scientific Reports*, 2015, **5**, 11773.
144. J. Schmidtke, W. Stille, H. Finkelmann and S. T. Kim, *Advanced Materials*, 2002, **14**, 746-749.
145. H. K. Bisoyi and Q. Li, *Chem Rev*, 2016, **116**, 15089-15166.
146. A. Varanytsia, H. Nagai, K. Urayama and P. Palffy-Muhoray, *Scientific reports*, 2015, **5**, 1-8.

147. M. Moirangthem and A. P. H. J. Schenning, *ACS Applied Materials and Interfaces*, 2018, **10**, 4168-4172.
148. I. Dierking, *Materials* 2014, **7**, 3568-3587.
149. B. Makowski, J. Kunzelman and C. Weder, *Handbook of Stimuli-Responsive Materials*, 2011, pp 117-138.
150. C. T. Nguyen, T. H. Tran, X. Lu and R. M. Kasi, *Polym. Chem.*, 2014, **5**, 2774-2783.
151. A. M. Lowe and N. L. Abbott, *Chem Mater*, 2012, **24**, 746-758.

TOC Picture

